Cell Reports, Volume *30*

Supplemental Information

APOL1 C-Terminal Variants May Trigger Kidney Disease through Interference with APOL3 Control of Actomyosin

Sophie Uzureau, Laurence Lecordier, Pierrick Uzureau, Dorle Hennig, Jonas H. Graversen, Fabrice Homblé, Pepe Ekulu Mfutu, Fanny Oliveira Arcolino, Ana Raquel Ramos, Rita M. La Rovere, Tomas Luyten, Marjorie Vermeersch, Patricia Tebabi, Marc Dieu, Bart Cuypers, Stijn Deborggraeve, Marion Rabant, Christophe Legendre, Søren K. Moestrup, Elena Levtchenko, Geert Bultynck, Christophe Erneux, David Pérez-Morga, and Etienne Pays

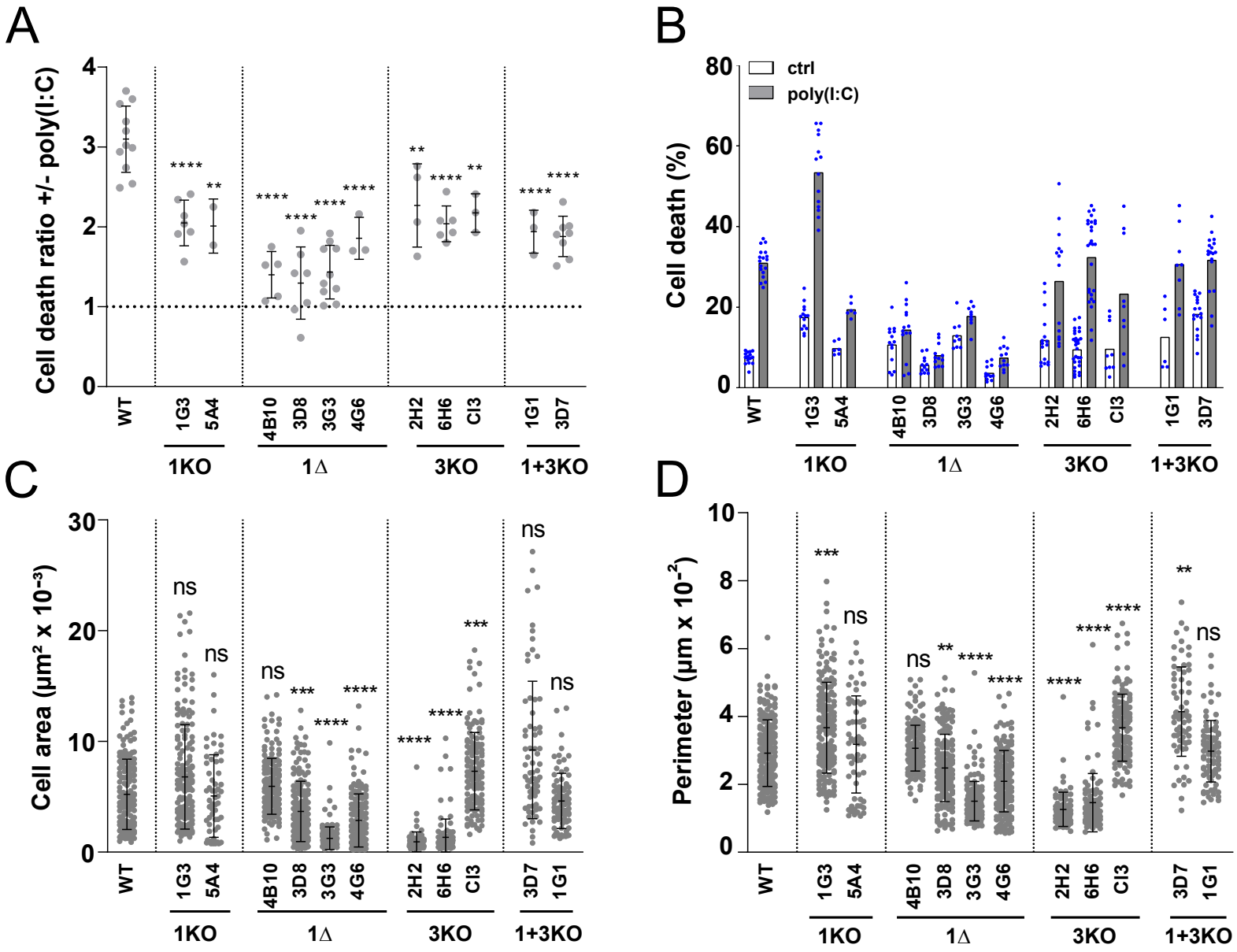
A
Cell death ratio +/- poly(I:C)
WT
1G3
5A4
4B10
3D8
3G3
4G6
2H2
6H6
Cl3
1G1
3D7
1KO
1Δ
3KO
1+3KO
B
ctrl
poly(I:C)
Cell death (%)
C
Cell area (µm² x 10⁻³)
D
Perimeter (µm x 10⁻²)
ns

Fig. S1

Figure S1. Editing of *APOL1* and/or *APOL3* affects the phenotype of independent podocyte clones (related to Figures 1 and 2)

(A) Poly(I:C)-induced cell death in different clones of the various podocyte lines. WT, n = 11; 1KO 1G3, n = 7; 1KO 5A4, n = 2; 1Δ 4B10, n = 5; 1Δ 3D8, n = 7; 1Δ 3G3, n = 10; 1Δ 4G6, n = 3; 3KO 2H2, n= 4; 3KO 6H6, n= 6; 3KO CI3, n= 3; 1+3KO 1G1, n = 3; 1+3KO 3D7, n = 8.

(B) Raw data of the poly(I:C)-mediated podocyte cell death measurements presented in Figs. 1C and Fig. S1A (ctrl= untreated control). Ctrl : WT, n = 15; 1KO 1G3, n = 14; 1KO 5A4, n = 6; 1Δ 4B10, n = 14; 1Δ 3D8, n = 12; 1Δ 3G3, n = 9; 1Δ 4G6, n = 12; 3KO 2H2, n= 16; 3KO 6H6, n= 28; 3KO CI3, n= 9; 1+3KO 1G1, n = 6; 1+3KO 3D7, n = 16. Poly(I:C) : WT, n = 18; 1KO 1G3, n = 14; 1KO 5A4, n = 6; 1Δ 4B10, n = 14; 1Δ 3D8, n = 12; 1Δ 3G3, n = 9; 1Δ 4G6, n = 12; 3KO 2H2, n= 16; 3KO 6H6, n= 28; 3KO CI3, n= 9; 1+3KO 1G1, n = 8; 1+3KO 3D7, n = 16.

(C) Cellular area of the different podocyte cell lines. WT, n = 179; 1KO 1G3, n = 168; 1KO 5A4, n = 61; 1Δ 4B10, n = 159; 1Δ 3D8, n = 157; 1Δ 3G3, n = 161; 1Δ 4G6, n = 158; 3KO 2H2, n= 87; 3KO 6H6, n= 102; 3KO CI3, n= 130; 1+3KO 3D7, n = 68; 1+3KO 1G1, n = 84.

(D) Cellular perimeter of the different podocyte cell lines. Same n values as panel C.

All quantitative results are expressed as means +/- SD.

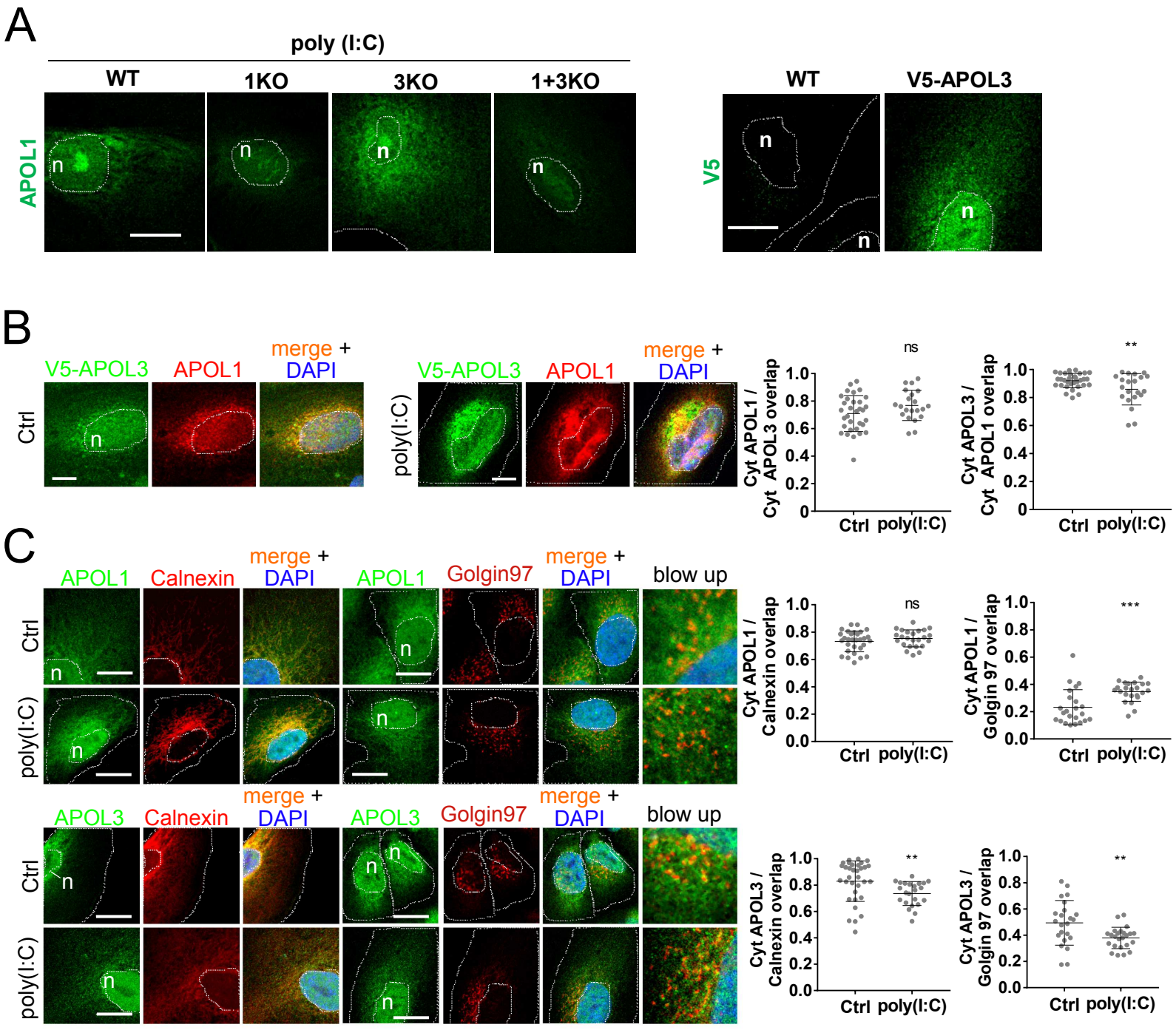
A
poly (I:C)
WT
1KO
3KO
1+3KO
APOL1
n
WT
V5-APOL3
V5
B
V5-APOL3
APOL1
merge + DAPI
Ctrl
poly(I:C)
Cyt APOL1 / Cyt APOL3 overlap
Cyt APOL3 / Cyt APOL1 overlap
ns
**
Ctrl
poly(I:C)
C
APOL1
Calnexin
Golgin97
blow up
Cyt APOL1 / Calnexin overlap
Cyt APOL1 / Golgin 97 overlap
***
APOL3
Cyt APOL3 / Calnexin overlap
Cyt APOL3 / Golgin 97 overlap

Fig. S2

Figure S2. APOL1 and APOL3 exhibit important co-localization with ER and Golgi membranes (related to Figures 1 and 2)

(A) Specificity of the immunolabelling with the anti-APOL1 and anti-V5 antibodies, as revealed by the strong reduction of staining, particularly cytoplasmic, with the anti-APOL1 antibody in the APOL1KO or APOL1+3KO cells, and by the absence of staining with the anti-V5 antibody in non-V5 tagged WT cells. Anti-V5 antibodies label C-terminal V5-tagged APOL3.

(B) Immunofluorescence analysis of APOL1 and APOL3 co-localization. The graphs show the co-localization levels of cytoplasmic APOL1 and V5-APOL3, following removal of the APOL staining covered with the nuclear DAPI marker (error bars = SD). ctrl, n = 32; poly(I:C), n = 21.

(C) Immunofluorescence analysis of APOL1 and APOL3 distribution with respect to ER and *trans*-Golgi markers (Calnexin and Golgin97, respectively). The graphs show the co-localization levels of cytoplasmic APOLs with ER or *trans*-Golgi markers, following removal of the APOL staining covered with the nuclear DAPI marker (error bars = SD). CytAPOL1/ Calnexin panel : ctrl, n = 30; poly(I:C), n = 24. CytAPOL1/ Golgin97 panel : ctrl, n = 23; poly(I:C), n = 23. CytAPOL3/ Calnexin panel : ctrl, n = 33; poly(I:C), n = 23. CytAPOL3/ Golgin97 panel : ctrl, n = 23; poly(I:C), n = 24.

Cells were randomly selected from 3 independent experiments (ctrl = untreated cells; n = nucleus; scale bars = 20 μm). In all images, the nuclear and cellular contours are indicated by dotted lines; when absent, these contours are outside the image surface.

APOL1

CRISPR

MEGAALLRVSVLCIWMSALFLGVRVRAEEAGARVQQNVPSGTDTGDPQSKPLGDWAAGTMDPESSIFIEDAIKYFKEKVSIQNLLLLLTDNEAWNGFVAAAE
LPRNEADELRKALDNLARQMIMKDKNWHDKGQQYRNWFLKEFPRLKSKLEDNIRRLRALADGVQKVHKGTTIANVVSGSLSISSGILTLVGMGLAPFTEGGS
LVLLEPGMELGITAALTGITSSTIDYGKKWWTQAQAHDLVIKSLDKLKEVKEFLGENISNFLSLAGNTYQLTRGIGKDIRALRRARANLQSVPHASASRPRV
TEPISAESGEQVERVNEPSILEMSRGVKLTDVAPVSFFLVLDVVYLVYESKHLHEGAKSETAEELKKVAQELEEKLNILNNNYKILQADQEL

CRISPR

APOL3

CRISPR

MDSEKKRFTEEATKYFRERVSPVHLQILLTNNEAWKRFVTAAELPRDEADALYEALKKLRTYAAIEDEYVQQKDEQFREWFLKEFPQVKRKIQESIEKLRAL
ANGIEEVHRGCTISNVVSSSTGAASGIMSLAGLVLAPFTAGTSLALTAAGVGLGAASAVTGITTSIVEHSYTSSAEAEASRLTATSIDRLKVFKEVMRDITP
NLLSLLNNYYEATQTIGSEIRAIRQARARARLPVTTWRISAGSGGQAERTIAGTTRAVSRGARILSATTSGIFLALDVVNLVYESKHLHEGAKSASAEELRR
QAQELEENLMELTQIYQRLNPCHTH

Cell line	Allele 1	Allele 2
APOL1KO clone 1G3	RVQQNVPSGTDTGDPQSKPLG ALGCWHHGPR *	RVQQNVPSGTDTGDPQSKPLG ALGCWHHGPR *
APOL1KO clone 5A4	RVQQNVPSGTDTGDPQSKPLGD KFTPLILTL *	WT
APOL1Δ clone 4B10	VLDVVYLVL RIKALT*	VLDVVYLVL RIKALT*
APOL1Δ clone 3D8 (hom)	VLDVVYLV RIKALT*	VLDVVYLV VRIKALT*
APOL1Δ clone 3G3 (het)	VLDVVYLV- SKHLHEGAKSETAEELKKVAQELEEKLNILNNNYKILQADQEL*	VLDVVYLV VRIKALT*
APOL1Δ clone 4G6	VLDVVYLV QSTYMRGQSQRQLRS*	VLDVVYLV QSTYMRGQSQRQLRS*
APOL3KO clone 2H2	DEADALYEALKKLRTYAA SRMFPVIQPLPLSLPILHTGPICPVRT*	DEADALYEALKKLRTYAA SRMFPVIQPLPLSLPILHTGPICPVRT*
APOL3KO clone 6H6	DEADALYEALKKLRT MRTNMCSRKMSSLGNGF*	DEADALYEALKKLRT FRTNMCSRKMSSLGNGF*
APOL3KO clone 3	DEADALYEALKKLRTYAA IEDEYVQQKDEQFREWFLKEFPQVKR KIQESIEKLRALANGIEEVHRGCTISNVVSSSTGAASGIMSLAGLV LAPFTAGTSLALTAAGVGLGAASAVTGITTSIVEHSYTSSAEAEAS RLTATSIDR *	DEADALYEALKKLRTYAA IEDEYVQQKDEQFREWFLKEFPQVKR KIQESIEKLRALANGIEEVHRGCTISNVVSSSTGAASGIMSLAGLV LAPFTAGTSLALTAAGVGLGAASAVTGITTSIVEHSYTSSAEAEAS RLTATSIDR *
APOL1KO (1G3) + APOL3KO clone 1G1	DEADALYEALKKLRTYA *	DEADALYEALKKLRTYA *
APOL1KO (1G3) + APOL3KO clone 3D7	DEADALYKKLRTYAA PRPLAPSPKPPDSPLQALPCPPHPLRLQV SSTSSSRCDD*	DEADALYKKLRTYAA PRPLAPSPKPPDSPLQALPCPPHPLRLQV SSTSSSRCDD*

Fig. S3

Figure S3. CRISPR/Cas9 editing of podocytes (related to all Figures)

In the APOL1 and APOL3 sequences, the coloured sections were edited in different podocyte cell lines as shown in the table.

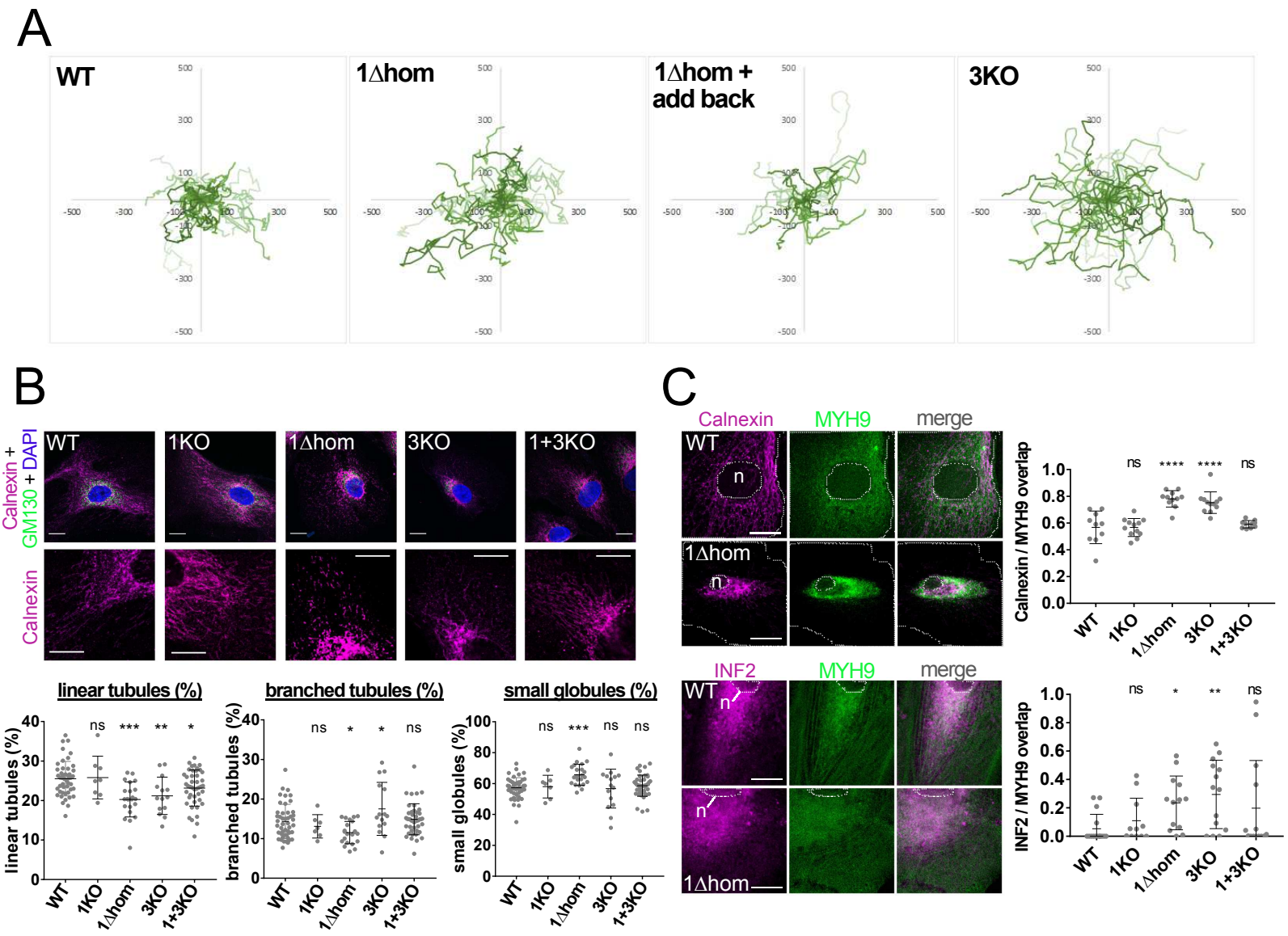
A
WT
1Δhom
1Δhom +
add back
3KO
B
Calnexin +
GM130 + DAPI
Calnexin
WT
1KO
1Δhom
3KO
1+3KO
linear tubules (%)
branched tubules (%)
small globules (%)
C
Calnexin
MYH9
merge
INF2
Calnexin / MYH9 overlap
INF2 / MYH9 overlap

Fig. S4

Figure S4. Effect of *APOL* editing on actomyosin organization: additional information (related to Figure 2)

(A) Cellular motility, as determined by single cell tracking of 30 randomly selected podocytes. The mobility of APOL1Δhom podocytes was analysed following or not doxycycline-inducible addback expression of WT APOL1.

(B) ER shape, as determined by measurement of calnexin-immunostained structures using MicroP software. WT, n = 47; 1KO, n = 8; 1Δhom, n = 22; 3KO, n= 14; 1+3KO, n = 44.

(C) Relative co-localization of the ER marker calnexin and INF2 with MYH9. Calnexin / MYH9 panel: WT, n = 10; 1KO, n = 11; 1Δhom, n = 12; 3KO, n= 12; 1+3KO, n = 10. INF2 / MYH9 panel: WT, n = 16; 1KO, n = 13; 1Δhom, n = 11; 3KO, n= 14; 1+3KO, n = 14.

Size bars = 2 µm. All quantitative measurements are expressed as means +/- SD.

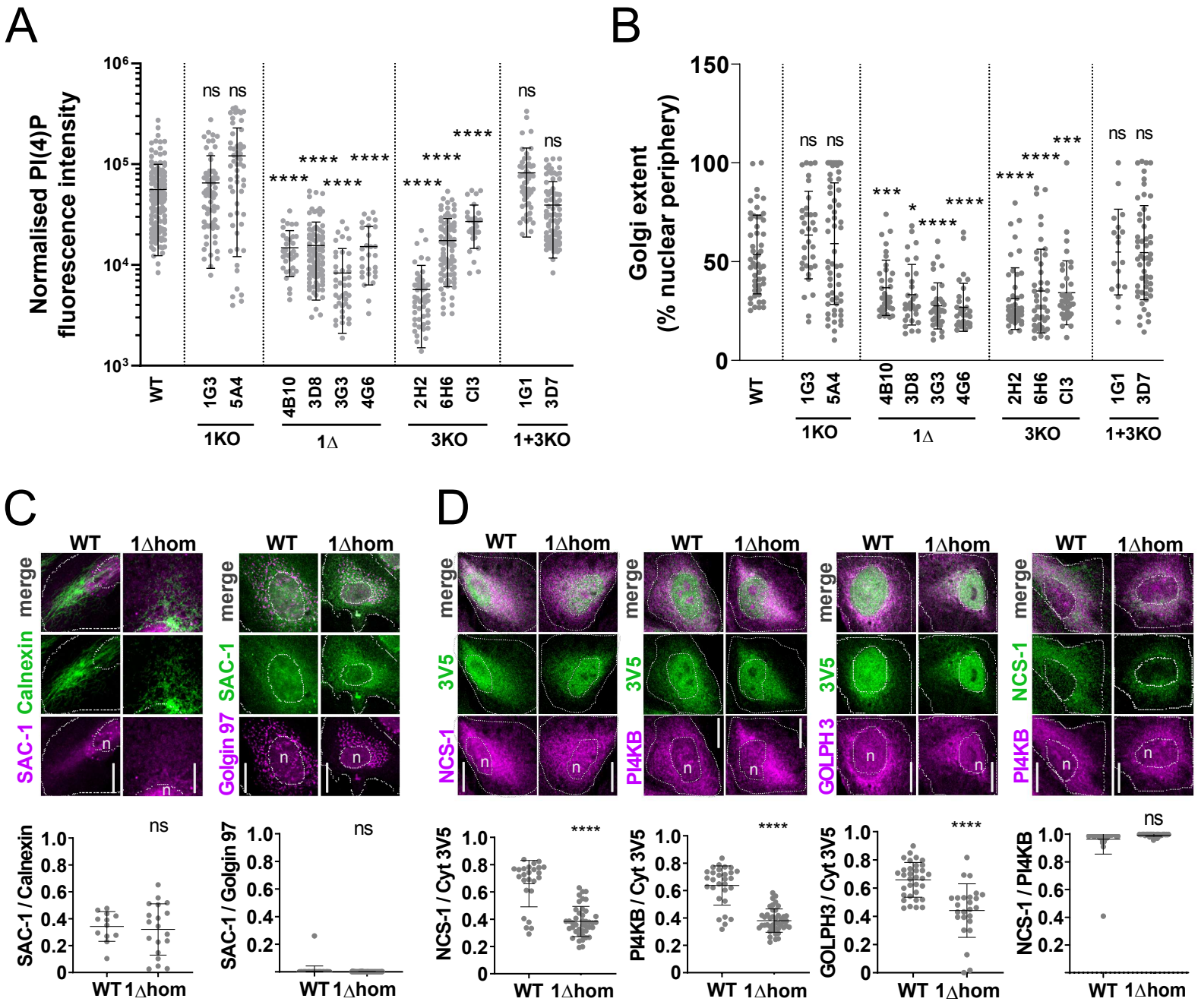
A
Normalised PI(4)P fluorescence intensity
WT
1G3
5A4
4B10
3D8
3G3
4G6
2H2
6H6
Cl3
1G1
3D7
1KO
1Δ
3KO
1+3KO
ns
****
B
Golgi extent (% nuclear periphery)
***
*
C
D
WT
1Δhom
merge
Calnexin
SAC-1
Golgin 97
3V5
NCS-1
PI4KB
GOLPH3
SAC-1 / Calnexin
SAC-1 / Golgin 97
NCS-1 / Cyt 3V5
PI4KB / Cyt 3V5
GOLPH3 / Cyt 3V5
NCS-1 / PI4KB

Fig. S5

Figure S5. Effect of *APOL* editing on PI4KB activity: additional information (related to Figure 3)

(A) Relative PI(4)P content in different clones of the APOL1Δ and APOL3KO cell lines, as determined by immunofluorescence with anti-PI(4)P antibodies. WT, n = 51; 1KO 1G3, n = 34; 1KO 5A4, n = 60; 1Δ 4B10, n = 34; 1Δ 3D8, n = 30; 1Δ 3G3, n = 35; 1Δ 4G6, n = 32; 3KO 2H2, n= 45; 3KO 6H6, n= 43; 3KO CI3, n= 38; 1+3KO 1G1, n = 18; 1+3KO 3D7, n = 53.

(B) Relative Golgi extent in different clones of the APOL1Δ and APOL3KO cell lines, as determined by immunofluorescence with anti-Golgin97 antibodies. WT, n = 143; 1KO 1G3, n = 68; 1KO 5A4, n = 55; 1Δ 4B10, n = 34; 1Δ 3D8, n = 92; 1Δ 3G3, n = 41; 1Δ 4G6, n = 28; 3KO 2H2, n= 49; 3KO 6H6, n= 83; 3KO CI3, n= 31; 1+3KO 1G1, n = 51; 1+3KO 3D7, n = 82.

(C) Relative co-localization of the PI(4)P phosphatase SAC-1 with the ER marker Calnexin and *trans*-Golgi marker Golgin97 in WT and APOL1Δ cells. SAC-1 / Calnexin panel: WT, n = 12; 1Δhom, n = 19. SAC-1 / Golgin97 panel: WT, n = 49; 1Δhom, n = 55.

(D) Relative co-localization of NCS-1, PI4KB and the *trans*-Golgi marker GOLPH3 with cytoplasmic V5-tagged APOL3, and between NCS-1 and PI4KB in WT and APOL1Δ cells. NCS-1 / Cyt 3V5 panel: WT, n = 25; 1Δhom, n = 42. PI4KB / Cyt 3V5 panel: WT, n = 29; 1Δhom, n = 43. GOLPH3 / Cyt 3V5 panel: WT, n = 33; 1Δhom, n = 25. NCS-1 / PI4KB panel: WT, n = 30; 1Δhom, n = 41.

Size bars = 2 µm. All quantitative measurements are expressed as means +/- SD.

A

Protein	Uniprot Reference	Molecular weight	WT	WT + poly (I:C)	1KO	1KO + poly (I:C)	1Δhom	1Δhom + poly (I:C)	3KO	3KO + poly (I:C)
MYH9	P35579	216 kDa	28	89	11	25	33	88	7	85
MYO6	Q9UM54	145 kDa	0	36	0	0	0	17	0	11
MYO1C	O00159	122 kDa	4	18	0	2	4	9	0	5
Gelsolin	B7Z6N2	85 kDa	2	17	0	0	8	11	0	10
Drebrin	Q16643	71 kDa	0	14	0	0	0	6	0	5
MYL9 or MYL12A (RLC)	Q6IBG1/J3QRS3	20 kDa/20 kDa	2	11	0	5	5	15	6	10
Coatomer subunit alpha	P53621	138 kDa	4	10	0	0	2	6	0	0
MYO5B	Q9ULV0	214 kDa	0	10	0	0	0	7	0	0
Tropomyosin (unique peptides)	see panel B	12 kDa	2	8	0	0	22	76	3	48
Protein phosphatase 1 regulatory subunit	B2RAH5	115 kDa	0	8	0	0	0	7	0	0
MYL6 (ELC)	H0YI43	29 kDa	6	7	0	6	8	14	4	11
MYO1D	O94832	116 kDa	2	7	0	0	0	5	0	7
Leucine-rich repeat flightless-interacting protein 2	Q9Y608	82 kDa	0	7	0	0	0	4	0	0
MYO1E	Q12965	127 kDa	5	6	4	6	0	2	0	0
Myosin phosphatase Rho-interacting protein (MPRIP)	H0Y2S9	203 kDa	0	5	0	0	0	10	0	5
Protein flightless-1 homolog	Q13045	145 kDa	0	5	0	0	0	2	0	0
collagen alpha-1(I) chain	P02452	133 kDa	0	5	0	0	0	0	0	0
60S ribosomal protein L28	H0YKD8	19 kDa	2	4	0	0	3	4	0	2
Ankycorbin	Q9P0K7	110 kDa	0	4	0	0	2	13	0	3
Coatomer subunit beta	P35606	102 kDa	0	4	0	0	0	4	0	0
Apolipoprotein L 1 (APOL1)	B2R9E5	41/38 kDa	0	4	0	0	0	2	2	9

B

	Uniprot Reference	WT	WT + poly (I:C)	1KO	1KO + poly (I:C)	1Δhom	1Δhom + poly (I:C)	3KO	3KO + poly (I:C)
tropomyosin alpha-3 chain isoform Tpm3.1cy	B2RDE1	0	4	0	0	4	23	0	14
tropomyosin alpha-4 chain isoform Tpm4.2cy	B4DVY2	2	5	0	0	7	18	0	14
tropomyosin beta chain isoform Tpm2.4	B4E3P1	0	0	0	0	0	19	0	14
Tropomyosin alpha-1 chain isoform Tpm1.9cy	H7BYY1	0	0	0	0	0	26	0	17
tropomyosin beta chain isoform Tpm2.3	P07951-3	0	0	0	0	0	15	0	11
tropomyosin alpha-1 chain isoform Tpm1.3sm	P09493-8	0	0	0	0	9	27	0	15

C

GO biological process	Fold enrichment	+/-	P Value
Actin filament-based process (GO:0030029)	13.87	+	5.02E-04
Vesicle-mediated transport (GO:0016192)	5.86	+	1.41E-03
Cellular localization (GO:0051641)	5.76	+	8.68E-05

GO molecular function	H. sapiens	Found	Expected	enrichment	+/-	P value
Microfilament motor activity	22	6	0.03	>100	+	6.04E-10
Actin-dependent ATPase activity	12	3	0.01	>100	+	1.11E-03
Motor activity	135	6	0.16	37.28	+	2.96E-05
Actin filament binding	137	6	0.16	36.74	+	3.22E-05
Calmodulin binding	188	7	0.22	31.23	+	5.06E-06
Actin binding	404	11	0.48	22.84	+	1.23E-09
Cadherin binding	294	7	0.35	19.97	+	1.07E-04
Cell adhesion molecule binding	449	7	0.54	13.08	+	1.84E-03
Cytoskeletal protein binding	853	11	1.02	10.82	+	3.44E-06
Unclassified	3792	2	5.52	0.44	-	0.00E00

Fig. S6

Figure S6. APOL1 is associated with actomyosin components (related to Figure 2)

(A) Mass spectrometry analysis of proteins co-immunoprecipitated with anti-APOL1 antibodies in different podocyte cell lines, incubated or not with poly(I:C). The immunoprecipitates were treated with 1% NP-40.

(B) Details of tropomyosin isoforms immunoprecipitated with APOL1 (peptides common to different isoforms are listed several times).

(C) Functional analysis of immunoprecipitated components.

A

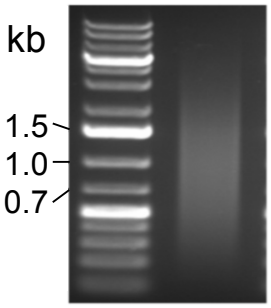

B

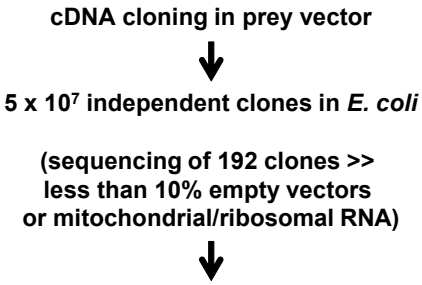

C

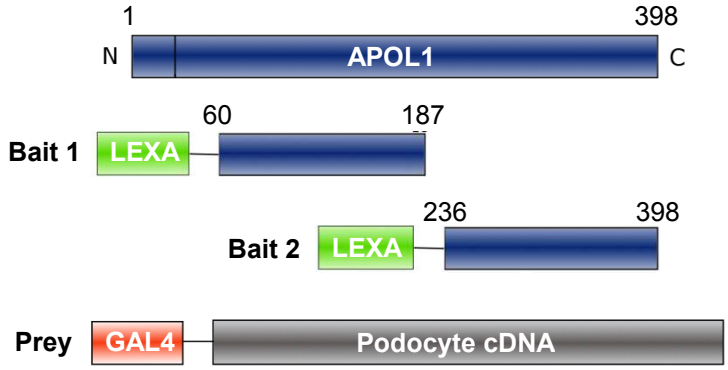

D

Bait 1

Gene name	score	SID (amino acid)	times found
APOL1	A	346-390	173
APOL2	A	267-326	155
BAIAP2	B	62-149	6
APOL3	C	263-327	2
COG4	D	1-109	1
CTNNAL1	D	318-427	1
DGCR14	D	24-97	1
GOLGA2	D	393-553	1
LAMB3	D	838-1074	1
MSC	D	13-206	2
STX12	D	131-222	2
STX1B	D	124-275	1

Bait 2

Gene name	score	SID (amino acid)	times found
APOL1	A	78-121	268
APOL2	B	1-114	16
APOL6	D	8-153	2
DNAJC14	D	530-672	1
DST	D	4145-4355	1
IPO4	D	303-420	2
LAMB1	D	1605-1765	2
LAMB2	D	1690-1798	1
LAMB3	D	826-1058	2
OSBPL9	D	1-20	3
PDXDC1	D	524-661	1
PKM	D	211-269	2
VCL	D	2-159	1

E

APOL1 SID1 (78-121): KVSIQNLLLLLTDNEAWNGFVAAAELPRNEADELRKALDNLARQ

APOL2 (1-114): MNPESSIFIEDYLKYFQDQVSRENLLQLLTDDEAWNGFVAAAELPRDEADELRKALNKLASHMVMKDKNRHDKDQQHRQ WFLKEFPRLKRELEDHIRKLRALAEEVEQVHRGTT

APOL1 SID2 (346-390): VLDVVYLVYESKHLHEGAKSETAEELKKVAQELEEKLNILNNNYK

APOL2 (267-326): AMSRGTMIVGAATGGILLLLDVVSLAYESKHLLEGAKSESAEELKKRAQELEGKLNFLTK

hydrophobic cluster (HC) leucine zipper (LZ)

Fig. S7

Figure S7. Y2H screening for APOL1-interacting proteins mostly reveals intramolecular interactions (related to Figure 4)

(A) cDNA was synthesized on pooled poly(A)+ RNA (50:50) from untreated and poly(I:C)-treated podocytes.

(B) The podocyte cDNA library was cloned in a prey vector and transfected in *Saccharomyces cerevisiae*.

(C) Different regions of the APOL1 sequence in a bait vector were used for the screening of podocyte interacting sequences. For bait 1 and bait 2, respectively 57.5 million interactions in the presence of 5 mM HIS3 inhibitor 3-amino-1,2,4-triazole (3-AT) and 67.6 million interactions in 0.5 mM 3-AT were analysed.

(D) List of the genes identified following the screening with the different baits (SID = smallest interacting domain; score: A = very high, B = high, C = good and D = moderate confidence in the interaction).

(E) Sequence comparison of the APOL1 and APOL2 SIDs (asterisks = identical amino acids; underlined violet amino acids: hydrophobic residues in HCs; underlined pink amino acids: positions “a” and “d” of heptads in LZs).

A

Interaction Matrix				Selection Medium							
N° / Type		Bait*	Prey**	DO-2	DO-3	DO-3 + 1mM 3AT	DO-3 + 5mM 3AT	DO-3 + 10mM 3AT	DO-3 + 50mM 3AT	DO-3 + 100mM 3AT	DO-3 + 200mM 3AT
1	**Positive control**	smad	smurf	+	+	+	+	+	+	+	+
2	Negative control	pB27ø	pP7ø	+	-	-	-	-	-	-	-
3	Negative control	pB27ø	APOL1 Cter wt	+	-	-	-	-	-	-	-
4	Negative control	APOL1 Nter	pP7ø	+	-	-	-	-	-	-	-
5	Interaction	APOL1 Nter	APOL1 Cter wt	+	+	+	+	+	+	+	+
6	Negative control	pB27ø	APOL1 Cter Mut G1	+	-	-	-	-	-	-	-
7	Interaction	APOL1 Nter	APOL1 Cter Mut G1	+	+	+	+	+	+	+	+
8	Negative control	pB27ø	APOL1 Cter Mut G2	+	-	-	-	-	-	-	-
9	Interaction	APOL1 Nter	APOL1 Cter Mut G2	+	+	+	+	+	+/-	-	-

* APOL1 Nter : [aa 60-187]
** APOL1 Cter : [aa 236-398/396]

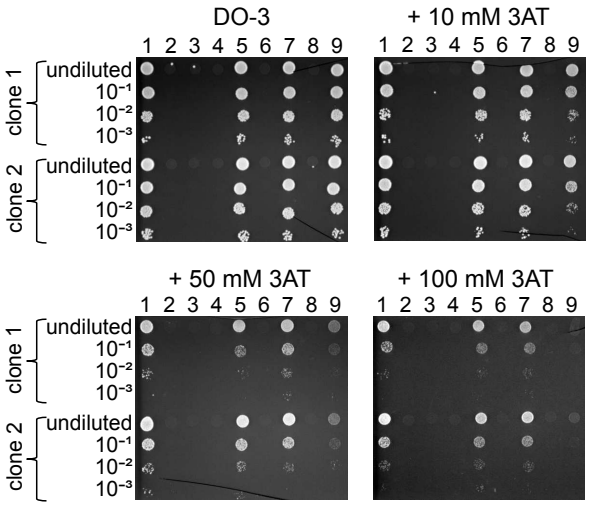

B

1	Positive control (smad /smurf)
2	Negative control (pB27o / pP7o)
3	Negative control (pB27o / APOL3 Cter)
4	Negative control (APOL1 Nter / pP7ø)
5	Interaction (APOL1 Nter / APOL3 Cter)

APOL1 Nter: aa 60-187
APOL3 Cter: aa 263-327

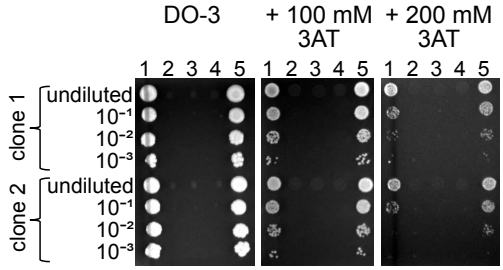

C

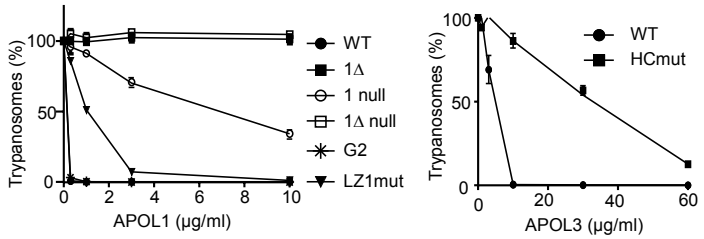

D

Interaction Matrix				Selection Medium	
N° / Type		Bait	Prey	DO-2	DO-3
1	Positive control	smad	smurf	+	+
2	Negative control	pB27ø	APOL1 Cter (339-390)	+	-
3	Negative control	APOL1 LZ1mut	pP7ø	+	-
4	Interaction	APOL1 LZ1mut	APOL1 Cter (339-390)	+	-
5	Negative control	pB27ø	APOL1 Cter (346-398)	+	-
6	Interaction	APOL1 LZ1mut	APOL1 Cter (346-398)	+	-
7	Negative control	pB27ø	APOL1 Cter (334-398)	+	-
8	Interaction	APOL1 LZ1mut	APOL1 Cter (334-398)	+	-

APOL1 LZ1mut: L111Q/L115Q/L118Q (aa 60-187)

E

Interaction Matrix				Selection Medium	
N° / Type		Bait	Prey	DO-2	DO-3
1	Positive control	smad	smurf	+	+
2	Negative control	APOL3 null mut	pP7ø	+	-
3	Negative control	APOL1 null mut	pP7ø	+	-
4	Negative control	APOL1Δ null mut	pP7ø	+	-
5	Negative control	pB27ø	NCS-1	+	-
6	Interaction	APOL3 null mut	NCS-1	+	+
7	Interaction	APOL1 null mut	NCS-1	+	-
8	Interaction	APOL1Δ null mut	NCS-1	+	-

APOL3 null mut: L137Q/A138Q/P139S/G143S
APOL1/1Δ null mut: P198S/G202S/G203S

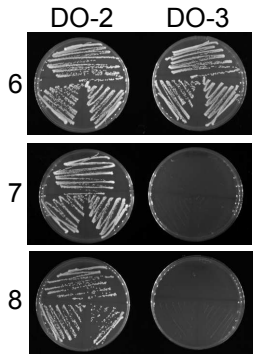

Fig. S8

Figure S8. APOLs interactions in the Y2H system: additional features (related to Figures 4 and S7)

(A) Strength of interactions between APOL1 SIDs, as measured by the resistance of the complexes to increasing concentrations of 3-AT. Positive and negative controls are indicated. Numbers above the lanes at the right correspond to those in the table at the left.

(B) Strength of interactions between SID1 and C-terminal APOL3 sequence, measured as in (A). Numbers above the lanes at the right correspond to those in the table at the left.

(C) Trypanolytic assays involving different APOL3 and APOL1 mutants used in this work, performed as a way to check protein activity following mutagenesis (means +/- SD; n = 3).

(D) Interactions between the 60-187 fragment of the LZ1mut mutant of APOL1 and different fragments containing SID2, all identified as strongly interacting with the 60-187 fragment of WT APOL1 in the initial cDNA library screening.

(E) Interactions of APOL3 or APOL1 null mutants with NCS-1. Numbers in the panel at the right correspond to those in the table at the left.

A

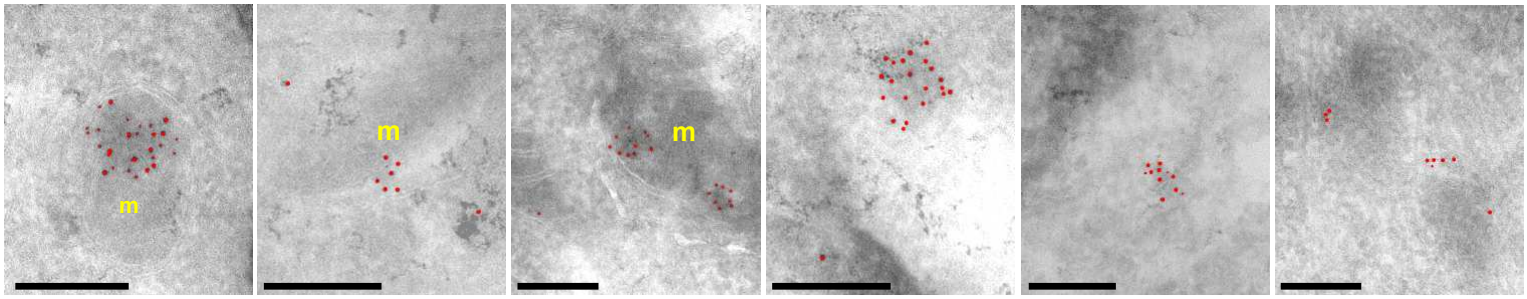
m
m
m

B

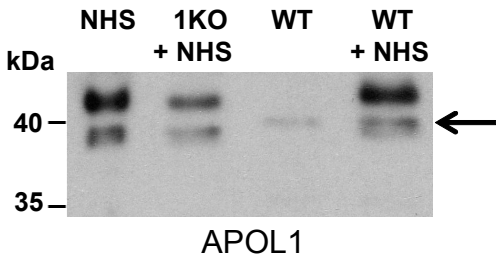
NHS
1KO
+ NHS
WT
WT
+ NHS
kDa
40
35
APOL1

C

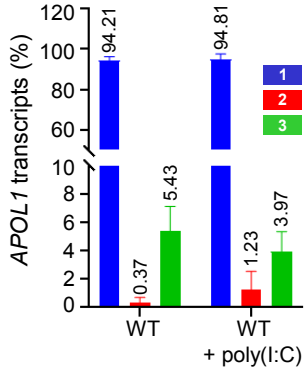
APOL1 transcripts (%)
120
100
80
60
10
8
6
4
2
0
94.21
0.37
5.43
94.81
1.23
3.97
1
2
3
WT
WT
+ poly(I:C)

D

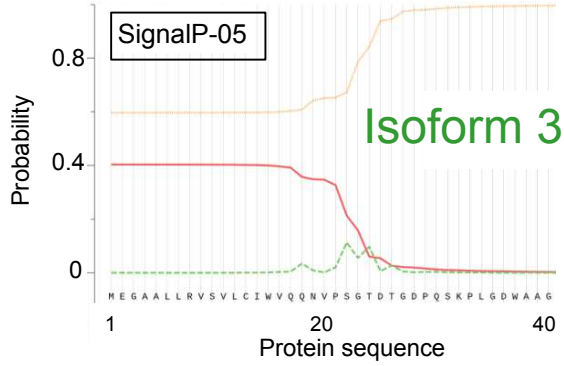
SignalP-05
Probability
0.8
0.4
0
Isoform 3
1
20
40
Protein sequence

E

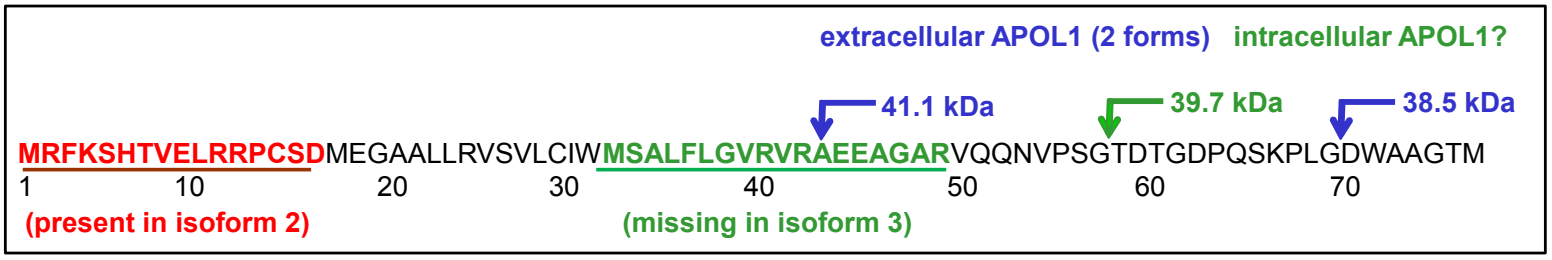
extracellular APOL1 (2 forms)
intracellular APOL1?
41.1 kDa
39.7 kDa
38.5 kDa
MRFKSHTVELRRPCSDMEGAALLRVSVLCIWMSALFLGVRVRAEEAGARVQQNVPSGTDTGDPQSKPLGDWAAGTM
1
10
20
30
40
50
60
70
(present in isoform 2)
(missing in isoform 3)

Fig. S9

Figure S9. Characterization of intracellular APOL1 (related to Figure 5)

(A) Immunogold detection of intracellular APOL1 in WT podocytes. Gold particles in the cytoplasm, which identify the localization of APOL1, were false-coloured in red. Control experiments on APOL1KO cells did not reveal any cytoplasmic labelling (not shown). Left panels illustrate clustered labelling close to the mitochondrion (m = mitochondrion); panels at the right exhibit cytosolic labelling. Bars = 200 nm.

(B) Western blot analysis of APOL1 in either normal human serum (NHS) (0.2 µl) or WT podocytes extracts (10 µg). NHS was added to extracts from either 1KO or WT podocytes to avoid any electrophoretic mobility difference linked to differential protein loading, also allowing the demonstration that intracellular APOL1 (arrow) migrates between the two APOL1 bands in NHS.

(C) qRT-PCR analysis of APOL1 isoforms (means +/-SD; n = 3).

(D) Prediction of signal peptide in APOL1 isoform 3, using the SignalP-5.0 program (Expasy).

(E) Comparison of the predicted cleavage sites in WT APOL1 (blue) or isoform 3 (green).

A

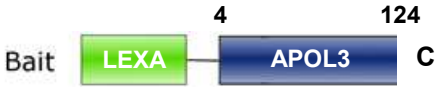

Gene name	score	SID (amino acid)	times found
PSME1	A	93-111	16
BCAR1	A	794-810	8
APOL1	B	367-392	5
APOL3	B	295-327	5
CAP1	B	15-78	6
HNRNPH1	B	36-245	6
LAMB1	B	1223-1279	3
ADAMTS1	C	205-288	3
BAP1	C	595-729	3
GDI2	C	370-445	5
NOP56	C	152-208	5
SPTBN1 var1	C	287-325 / 571-605 / 941-1023 / 1796-1936	9
UBAC1	C	28-312	4
WTAP	C	1-170	3
64 preys have been identified with score D			

B

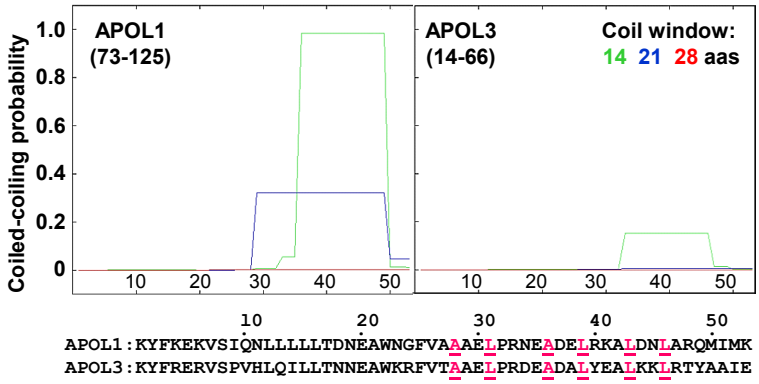

C

Gene name	score	SID (amino acid)	times found
NCS-1	A	17-189	33
PSMD2	A	461-619	18
TRIM8	A	210-302	7
AOE37-2	B	64-223	5
APOL1	C	57-164	2
CDC42BPB	D	23-171	2
HEG1	D	914-1148	1
HPCAL1	D	7-193	1
KCNIP1	D	53-227	4
PICALM	D	1-230	6
SP140L	D	252-499	1
YLPM1	D	1185-1469	1

Fig. S10

Figure S10. Y2H screening for APOL3-interacting proteins does not reveal intramolecular interaction, but identifies NCS-1 (related to Figures 4 and S7)

(A) Y2H screening experiment conducted with the 1-124 fragment of APOL3. 51.2 million interactions in 20 mM 3-AT were analysed. Score: A = very high, B = high, C = good and D = moderate confidence in the interaction

(B) Evaluation of the potential of APOL1 and APOL3 N-terminal regions to form coiled-coils (COILS program, Expasy). Pink colours highlight the amino acids at positions “a” and “d” of heptad repeats in LZs (see Fig. 4).

(C) Y2H screening experiment conducted with the complete sequence of the APOL3 null mutant (L137Q/A138Q/P139S/G143S) (Fontaine et al., 2017). 114 million interactions without 3AT were analysed. Same scores as in (A).

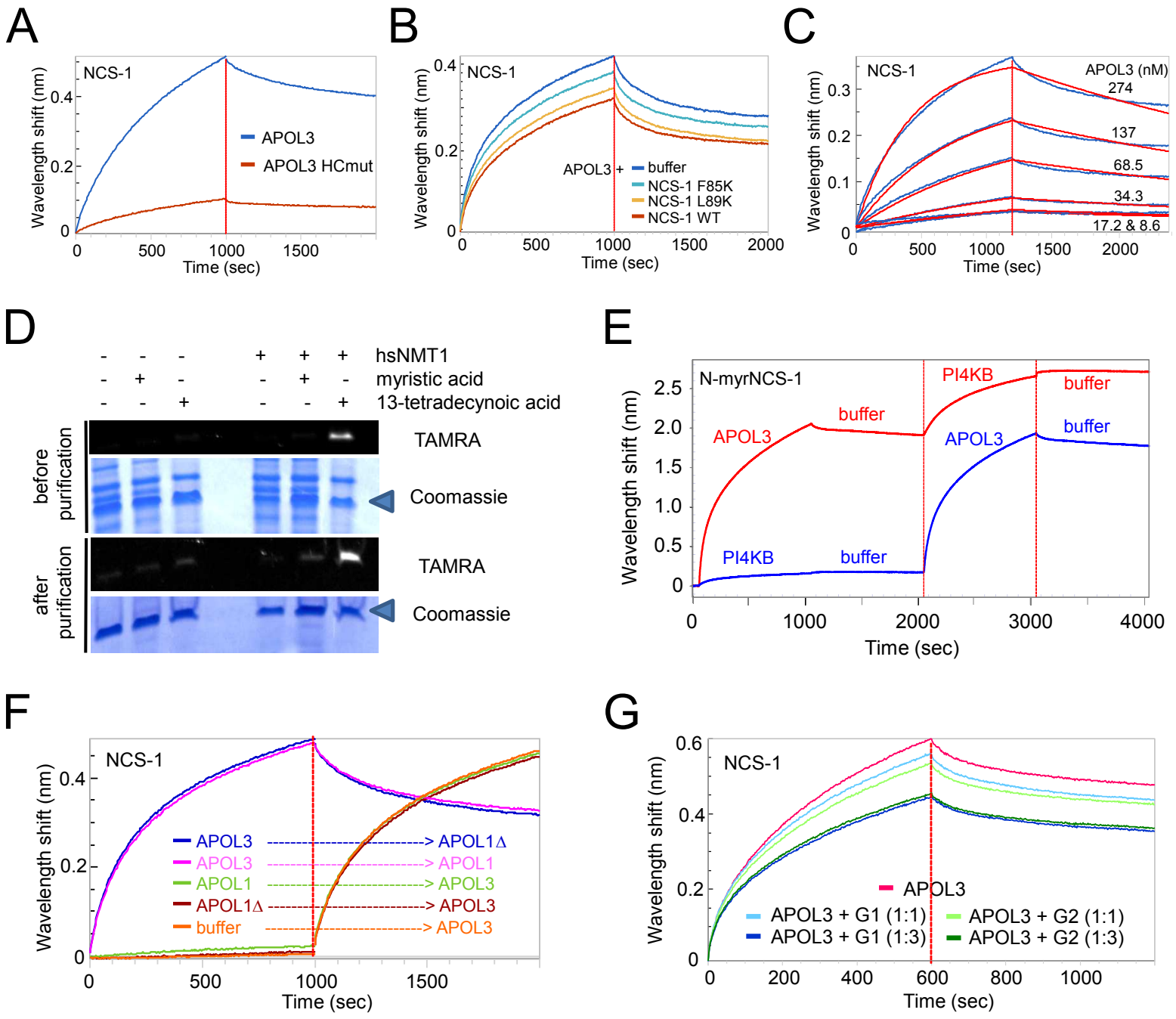
A
NCS-1
Wavelength shift (nm)
Time (sec)
APOL3
APOL3 HCmut
B
NCS-1
APOL3 +
buffer
NCS-1 F85K
NCS-1 L89K
NCS-1 WT
C
NCS-1
APOL3 (nM)
274
137
68.5
34.3
17.2 & 8.6
D
hsNMT1
myristic acid
13-tetradecynoic acid
TAMRA
Coomassie
before purification
after purification
E
N-myrNCS-1
PI4KB
buffer
APOL3
F
NCS-1
APOL3 -> APOL1Δ
APOL3 -> APOL1
APOL1 -> APOL3
APOL1Δ -> APOL3
buffer -> APOL3
G
NCS-1
APOL3
APOL3 + G1 (1:1)
APOL3 + G1 (1:3)
APOL3 + G2 (1:1)
APOL3 + G2 (1:3)

Fig. S11

Figure S11. Binding of APOL1 variants and NCS-1 to APOL3: additional features (related to Figure 5)

(A) BLI measurements of interaction between bound NCS-1 and APOL3 or APOL3 HC2-like mutant HCmut (n = 3).

(B) BLI measurements of interaction between bound NCS-1 and APOL3, in the presence or not of WT or mutant NCS-1 in a molar ratio of 1:2 (APOL3 : NCS-1) (n = 3).

(C) BLI measurements of interaction between bound NCS-1 and various concentrations of APOL3, with fitted curves (red) for determination of APOL3/NCS-1 binding affinity (n = 3).

(D) Generation of N-myristoylated NCS-1. Recombinant NCS-1 was synthesized in *E. coli* together or not with human N-myristoyl-transferase (hsNMT1) and either myristic acid or its alkynyled analogue 13-tetradecynoic acid. Fluorescent N-myristoylated NCS-1 was detected by binding of the TAMRA fluorophore to NCS-1-bound 13-tetradecynoic acid. Coomassie blue staining allows detection of NCS-1 (arrowhead), in total *E. coli* extracts or purified recombinant protein fraction.

(E) BLI measurements of interaction between bound N-myristoylated NCS-1 and APOL3 or PI4KB, added sequentially as indicated (n = 3).

(F) BLI measurements of interaction between bound NCS-1 and various APOLs, added sequentially as indicated (n = 3).

(G) BLI measurements of interaction between bound NCS-1 and APOL3, alone or with different molar ratios of G1 or G2 (n = 3).

All quantitative measurements are expressed as means +/- SD.

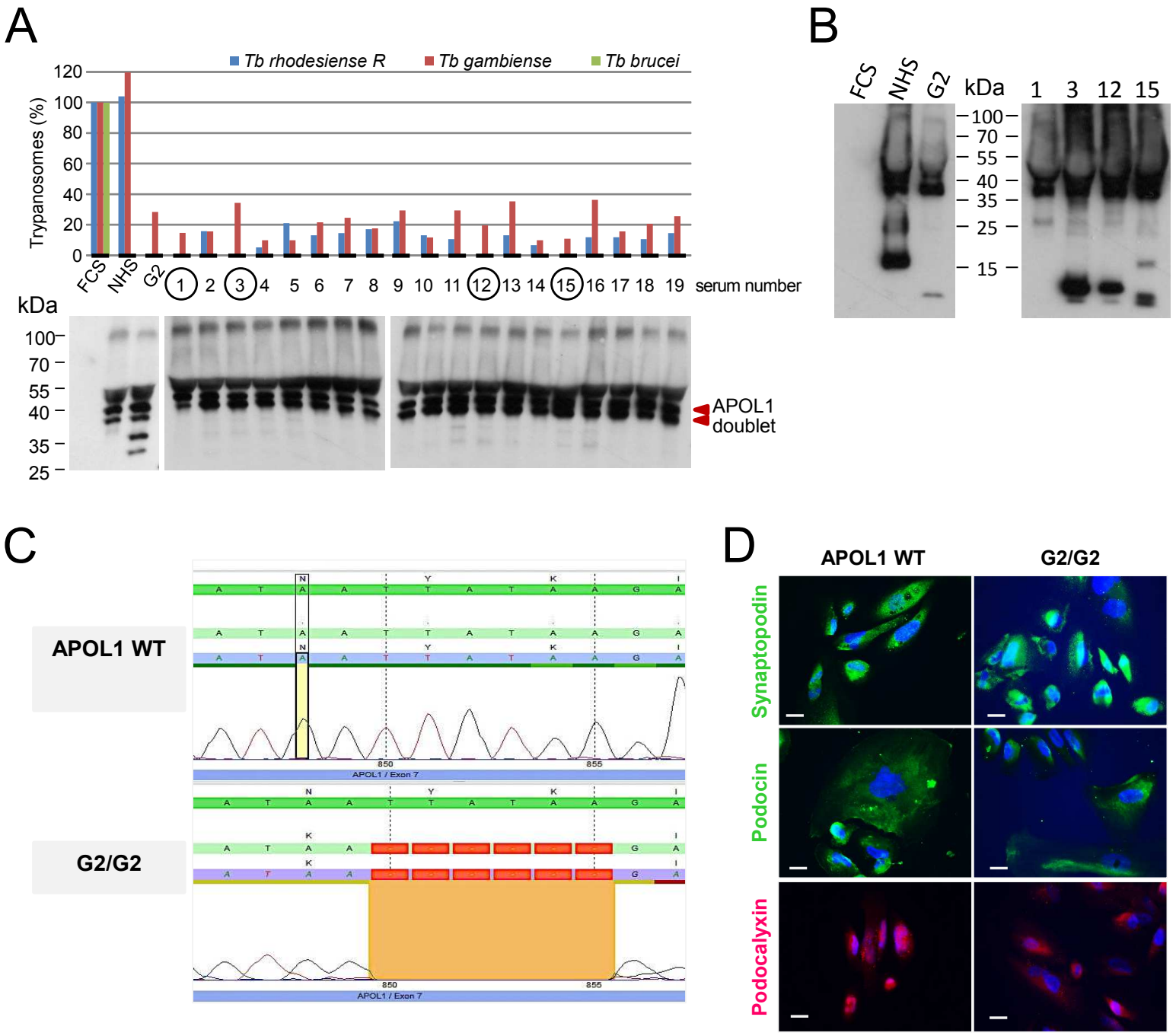
A
Tb rhodesiense R
Tb gambiense
Tb brucei
Trypanosomes (%)
120
100
80
60
40
20
0
FCS
NHS
G2
1 2 3 4 5 6 7 8 9 10 11 12 13 14 15 16 17 18 19
serum number
kDa
100
70
55
40
35
25
APOL1
doublet
B
FCS
NHS
G2
kDa
100
70
55
40
35
25
15
1 3 12 15
C
APOL1 WT
G2/G2
850
855
APOL1 / Exon 7
D
APOL1 WT
G2/G2
Synaptopodin
Podocin
Podocalyxin

Fig. S12

Figure S12. Generation of urine *APOL1* WT and *G2/G2* podocyte cell lines (related to Figure 7)

(A) Top panel: identification of WT and variant APOL1 genotypes by trypanolytic assays of different human sera on *T. rhodesiense*, *T. gambiense* and *T. brucei*. The parasites were incubated with 20% fetal calf serum (FCS), normal human serum (NHS) or G2 human serum, and with sera from humans with various APOL1 genotypes. The parasite growth ratio after overnight incubation is expressed as a percentage of control growth in FCS. Sera 1, 3, 12 and 15 (encircled) exhibited G1 or G2 phenotypes. Bottom panel: western blot serum analysis with anti-APOL1.

(B) Western blot sera analysis with anti-haptoglobin (Hp), meant to evaluate if Hp variation could explain the relative resistance to *T. rhodesiense* (Lecordier et al., 2015)

(C) Genotype of *APOL1 WT* and *G2/G2* podocytes upon amplification of exon 7.

(D) Immunofluorescence staining for podocyte-specific proteins synaptopodin, podocin and podocalyxin with the nuclear staining DAPI (blue). Scale bar: 50 μm.

A

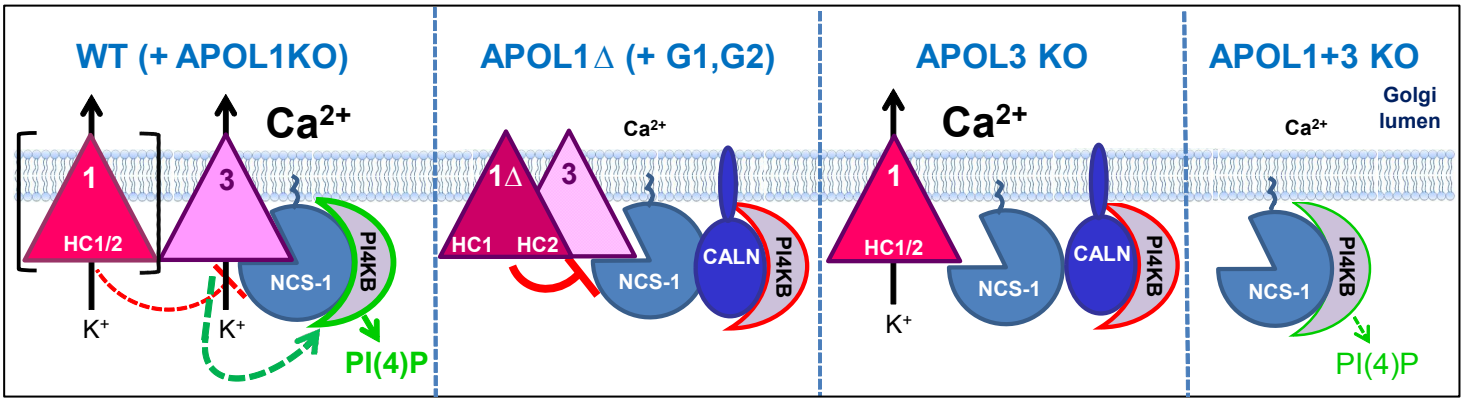
WT (+ APOL1KO)
APOL1Δ (+ G1,G2)
APOL3 KO
APOL1+3 KO
Ca2+
Golgi lumen
1
HC1/2
3
1Δ
HC1
HC2
NCS-1
CALN
PI4KB
K+
PI(4)P

B

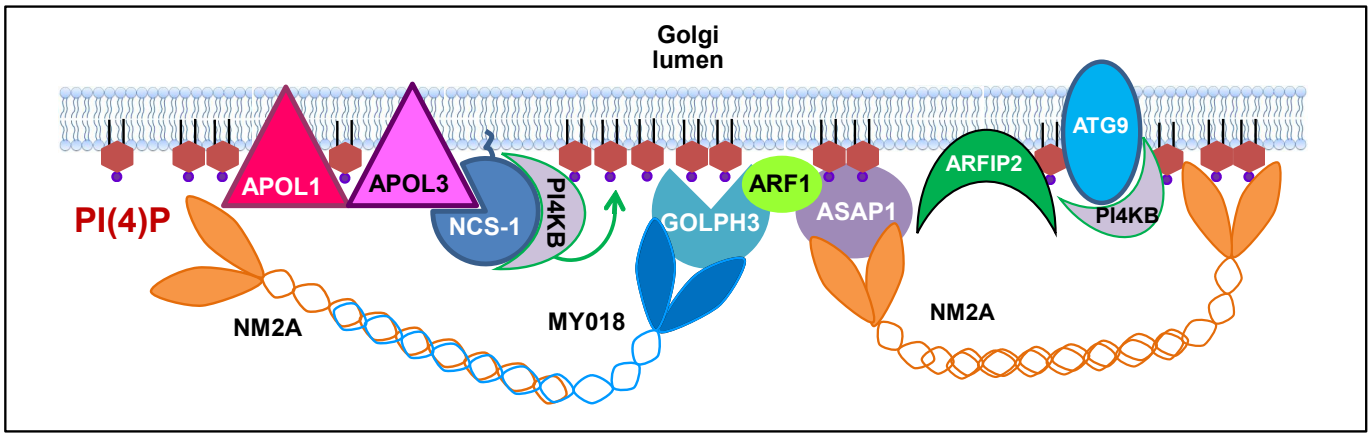
Golgi lumen
APOL1
APOL3
NCS-1
PI4KB
PI(4)P
GOLPH3
ARF1
ASAP1
ARFIP2
ATG9
NM2A
MY018

Fig. S13

Figure S13. Control of PI4KB and actomyosin by APOLs: a model (related to all Figures)

(A) APOL control of PI(4)P synthesis. APOL1 and APOL3 are inserted in the Golgi membrane where they can exhibit K^+ channel activity. PI4KB is anchored to Golgi membranes notably through interactions with the ACBD3/giantin complex (Klima et al., 2016) and synthesizes PI(4)P that is crucial for secretion (Bishé et al., 2012; de Barry et al., 2006; Dippold et al., 2009; Haynes et al., 2005; Kuna and Field, 2019; Tokuda et al., 2014; Zhao et al., 2001). The N-myristoylated form of NCS-1 activates PI4KB through a direct interaction (Zhao et al., 2001). APOL3 interacts with NCS-1 irrespective of NCS-1 myristoylation, through Ca^{2+}-dependent hydrophobic contacts involving its C-terminal hydrophobic cluster. These contacts evoke those between the yeast NCS-1 homologue Frq1 and the PI4KB homologue Pik1 (Pandalaneni et al., 2015; Strahl et al., 2003). Whereas APOL1 or APOL1 G1/G2 variants can hinder association of APOL3 with NCS-1 (dotted or plain red line respectively), APOL1Δ can bind to APOL3 and inactivate this protein without dissociating the APOL3/NCS-1 complex. In APOL1Δ and APOL3KO cells where APOL3 is no longer active, PI4KB is inhibited and the level of Golgi PI(4)P is reduced. However, in the absence of both APOL1 and APOL3, PI4KB appears to be active. In addition to the control of PI4KB, APOL1 and APOL3 also influence the levels of Ca^{2+} in Golgi stores, possibly through their redundant K^+ channel activity. Hypotheses attempting to explain these observations are presented in the discussion (CALN = PI4KB inhibitor calneuron).

(B) Interplay between APOLs, PI(4)P and the NM2A myosin. APOL1 and APOL3 bind to and co-localize with PI(4)P, and indirectly associate with the fission and secretion motor NM2A. Multiple pathways connect PI(4)P with NM2A. In particular, (i) the PI(4)P-binding protein GOLPH3 binds to the NM2A-interacting protein MYO18A (Billington et

al., 2015; Dippold et al., 2009; Kuna and Field, 2019; Taft et al., 2013), (ii) the phosphoinositide-binding GTPase-activating protein ASAP1 interacts with the ARF1-binder GOLPH3 and with NM2A (Chen et al., 2016; Kam et al., 2000; Rodrigues et al., 2016; Tu et al., 2012), (iii) the NM2A heavy chain MYH9 directly binds to anionic phospholipids (Liu et al., 2016), and (iv) PI4KIIIβ and PI4P initiate autophagy by recruiting ATG9, ARFIP2 and NM2A at the Golgi (Judith et al., 2019). Thus, affecting Golgi PI(4)P level influences actomyosin organization, vesicular trafficking and autophagy (review in Tan and Brill, 2014).

Table S1.
Genome sequencing of CRISPR/Cas9-generated podocyte clones (related to Fig. S3)

A. CRISPR/Cas9 target sites.

Target	Protospacer	PAM (-NGG)
APOL2	**T**GTGCTGCTGGTCTTTATCG	TGG
APOL3 **exon 5**	**T**AGAACATATGCAGCTATTG	AGG
APOL3 **exon 5**	**A**ACCAGCATTGACCGATTGA	AGG
APOL1 **exon 3**	**A**AGTAAGCCCCTCGGTGACT	GGG
APOL1 **exon 5**	**A**GTGCTTTGATTCGTACACG	AGG

B. Sequencing coverage of the podocyte genomes.

	WT	1KO	1Δhet	1Δhom	3KO
% cov. 10x	98,46	98,60	97,91	98,28	98,39
% cov. 20x	89,36	89,89	81,58	84,58	87,94
% cov. 30x	44,71	50,50	32,16	36,76	52,77
Average coverage	29,44	30,67	26,64	27,84	30,87
St. dev. coverage	34,97	36,45	32,88	34,18	35,88

C. Mutations in *APOL1* and *APOL3* detected following whole genome sequencing.

Sample	Gene	Position (chr22)	cDNA position	CDS position	Type	Modification
APOL1KO	*APOL1*	36257381	484/3017	210/1245	deletion	AC
APOL1KO	*APOL1*	36257381	484/3017	210/1245	insertion	C
APOL1Δhom	*APOL1*	36265858	1345/3017	1071/1245	deletion	TAAGCTTCTTTCTT GTGCTGGATGTA GTCTACCTCGTGT ACGAATCAAA
APOL1Δhom	*APOL1*	36265893	1382/3017	1108/1245	deletion	GT
APOL1Δhom	*APOL1*	36265895	1383/3017	1109/1245	insertion	G
APOL1Δhet	*APOL1*	36265895	1383/3017	1109/1245	insertion	G
APOL1Δhet	*APOL1*	36265895	1383/3017	1109/1245	deletion	GTACGA
APOL3KO	*APOL3*	36141621	827/2124	789/1209	deletion	A

D. On-target and off-target homozygous (minimal 10-fold coverage) and heterozygous (minimal 20-fold coverage) SNPs with moderate or high impact.

		1KO	**1Δhom**	**1Δhet**	**3KO**
Homozygous SNPs	Total number of SNPs (moderate impact/high impact)	0(0/0)	0(0/0)	3(0/0)	1(1/0)
	Genes affected by moderate or high impact SNPs				HEG1 (moderate impact)
Heterozygous SNPs	Total number of SNPs (moderate impact/high impact)	5140(12/0)	9133(18/1)	6605(21/1)	28007(88/4)
	Genes affected by high impact SNPs		ERBB3	IGSF1	C2orf91 HAAO DSCAM EXOC1

E. On-target and off-target homozygous (minimal 10-fold coverage) and heterozygous (minimal 20-fold coverage) INDELs with moderate or high impact.

		1KO	**1Δhom**	**1Δhet**	**3KO**
Homozygous INDELs	Total number of INDELs (moderate impact/high impact)	10(0/1)	23(0/1)	25(0/0)	21(0/1)
	Genes affected by moderate or high impact INDELs	**APOL1** (high impact)	**APOL1** (high impact)	/	**APOL3** (high impact)
Heterozygous INDELs	Total number of INDELs (moderate impact/high impact)	20542 (3/5)	15710 (4/9)	17545 (2/9)	23781 (5/4)
	Genes affected by high impact INDELs	PRPF3 GEMIN2 GOLGA6L2 ANKRD36 IL32	MED1 POT1 GOLGA6L2 ANKRD36 IL32 RUBCN ZNF879 TCEB3CL ZBTB10	MED1 POT1 GOLGA6L2 ANKRD36 LINC00368 TCEB3CL LOC63930 **APOL1** GEMIN2	MED1 POT1 GOLGA6L2 ANKRD36